Research Activities

– Off-line Experiments –

Inverse Photoemission Study on the Kitaev Material α-$RuCl_3$

Soobin Sinn[a,b], Choong Hyun Kim[a,b], Beom Hyun Kim[c,d], Kyung Dong Lee[e], Choong Jae Won[e], Ji Seop Oh[a,b], Moonsup Han[f], Young Jun Chang[f], Namjung Hur[e], Hitoshi Sato[g], Byeong-Gyu Park[h], Changyoung Kim[a,b], Hyeong-Do Kim[a,b], and Tae Won Noh[a,b],

[a]*Center for Correlated Electron Systems, Institute for Basic Science (IBS), Seoul 08826, Republic of Korea.*
[b]*Department of Physics and Astronomy, Seoul National University (SNU), Seoul 08826, Republic of Korea.*
[c]*Computational Condensed Matter Physics Laboratory, RIKEN, Wako, Saitama 351-0198, Japan.*
[d]*Interdisciplinary Theoretical Science (iTHES) Research Group, RIKEN, Wako, Saitama 351-0198, Japan.*
[e]*Department of Physics, Inha University, Incheon 22212, Republic of Korea.*
[f]*Department of Physics, University of Seoul, Seoul 02504, Republic of Korea.*
[g]*Hiroshima Synchrotron Radiation Center, Hiroshima University, Kagamiyama 2-313, Higashi-Hiroshima 739-0046, Japan.*
[h]*Pohang Accelerator Laboratory, Pohang University of Science and Technology, Pohang 37673, Republic of Korea.*

Keywords: Inverse photoemission spectroscopy, Kitaev spin liquid

Realizing the quantum spin liquid has been one of the central research interest of the condensed matter physics. It was theoretically suggested that the bond-dependent magnetic interaction called Kitaev interaction on a honeycomb lattice can stabilize the quantum-spin-liquid ground state [1,2]. Recently, honeycomb 4*d* compound α-$RuCl_3$ have been attracted attentions as potential candidates for the Kitaev spin liquid [3,4] because spin-orbit coupling of 4*d* transition-metal ion is a key requirement for the dominant Kitaev interaction [2]. To understand their strength of magnetic interactions and ground states, values of the physical parameters such as Coulomb interaction U and Hund Coupling J_H are important [5]. The parameters can be obtained from the electronic structure study. However, there have been little investigations on the electronic structure, compared to extensive studies on their magnetic properties. Photoemission and inverse photoemission spectroscopies can be direct tools for the purpose [6]. By comparing the result of the configuration-interaction calculations, the physical parameters, which explains their unconventional magnetic ground states, will be obtained. Figure 1 shows the inverse photoemission spectrum of α-$RuCl_3$. We observed two prominent peaks near the Fermi level corresponding to J_{eff} = 1/2 upper Hubbard band and Ru e_g band. An energy separation between the two peaks is about 2.2 eV, which is similar to 10 Dq value obtained from an x-ray absorption spectroscopy [7]. By analyzing this and the photoemission spectrum, we obtained electronic parameters and strengthes of exotic magnetic interactions of the material. [6]

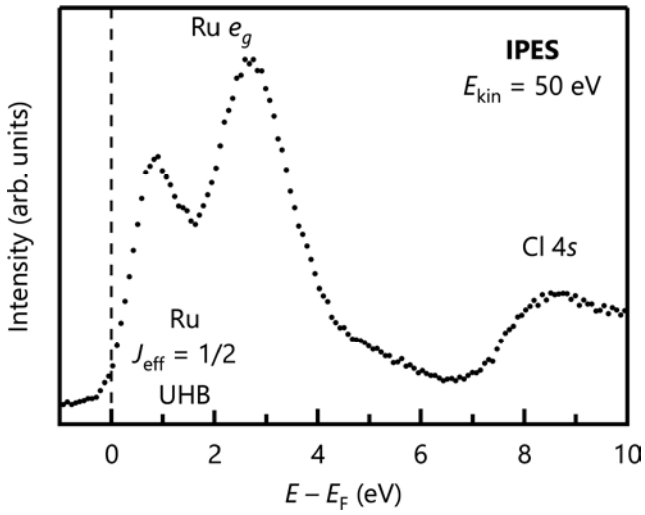

FIGURE 1. Inverse photoemission spectrum of α-$RuCl_3$.

REFERENCES

1. A. Kitaev, Ann. Phys. **321**, 2 (2006).
2. J. Chaloupka, G. Jackeli, and G. Khaliullin, Phys. Rev. Lett. **105**, 027204 (2010).
3. A. Banerjee *et al.*, Nat. Mater. **15**, 733 (2016).
4. J. Nasu *et al.*, Nat. Phys. **12**, 912 (2016).
5. J. G. Rau, E. K.-H. Lee, and H.-Y. Kee, Phys. Rev. Lett. **112**, 077204 (2014).
6. S. Sinn *et al.*, Sci. Rep. **6**, 39544 (2016).
7. K. W. Plumb *et al.*, Phys. Rev. B **90**, 041112 (2014).

Laser-based high-resolution angle-resolved photoemission study of $Bi_2Sr_2Ca(Cu_{1-x}Co_x)_2O_{8+\delta}$

T. Miyashita[a], W. Mansuer[a], H. Takita[a], T. Kubo[a], S. Ishizaka[b], E. F. Schwier[c], H. Iwasawa[c,d], K. Shimada[c], M. Arita[c], H. Namatame[c], Y. Numata[e], T. Uto[e], A. Matsuda[e], and A. Ino[a,c]

[a]*Graduate School of Science, Hiroshima University, Higashi-Hiroshima 739-8526, Japan*
[b]*Department of Physics, Hiroshima University, Higashi-Hiroshima 739-8526, Japan*
[c]*Hiroshima Synchrotron Radiation Center, Hiroshima University, Higashi-Hiroshima 739-0046, Japan*
[d]*Diamond Light Source, Harwell Campus, Didcot OX11 0DE, United Kingdom*
[e]*School of Advanced Science and Engineering, Waseda University, Shinjuku 169-8050, Japan*

Keywords: Angle-resolved photoemission spectroscopy, High-T_c cuprate, Superconducting gap, Impurity effect.

Conventional superconductivity occurs when electrons are coupled with each other to form Cooper pairs. It has been suggested that the pairing mechanism of high-T_c superconductivity in cuprate has some relation with antiferromagnetic fluctuation. However, it remains controversial. In order to clarify the pairing mechanism, the relationship between critical temperature T_c and superconducting gap Δ is important, because Δ represents the binding energy of a Cooper pair. Conventional mean-field theory predicts that T_c linearly scales with Δ [1]. In experiment, however, the relationship between T_c and Δ of the high-T_c cuprate has been unclear, because the nodal gap is smaller than the energy resolution of photoemission experiment. In addition, a pseudogap has also been observed above T_c around an antinode. In this study, we performed laser-based high-resolution angle-resolved photoemission (ARPES) experiment of $Bi_2Sr_2Ca(Cu_{1-x}Co_x)_2O_{8+\delta}$, and determined the directional dependence of near-nodal small gap. Comparing with the result of pristine cuprate, $Bi_2Sr_2CaCu_2O_{8+\delta}$, we discuss the effect of substituting magnetic element Co for Cu.

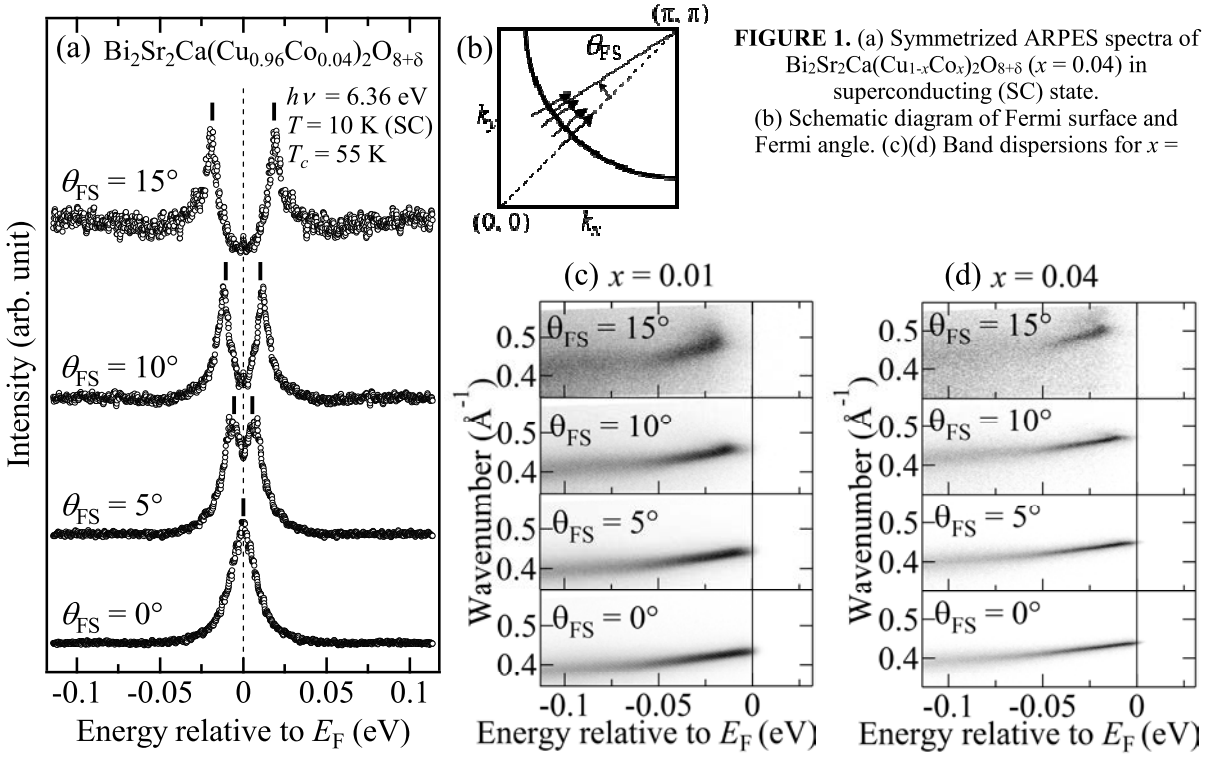

FIGURE 1. (a) Symmetrized ARPES spectra of $Bi_2Sr_2Ca(Cu_{1-x}Co_x)_2O_{8+\delta}$ (x = 0.04) in superconducting (SC) state. (b) Schematic diagram of Fermi surface and Fermi angle. (c)(d) Band dispersions for x =

Single crystals of $Bi_2Sr_2Ca(Cu_{1-x}Co_x)_2O_{8+\delta}$ (x = 0.01 and 0.04) were grown by traveling-solvent-floating-zone (TSFZ) method [2]. The excess oxygen δ was optimized by post annealing procedure so that critical temperature T_c is at the maximum, T_c = 80 K and 55 K, for x =0.01 and 0.04, respectively. Clean surfaces were obtained by *in situ* cleaving. High-resolution ARPES measurement was performed with laser light of $h\nu$ = 6.36 eV and a spectrometer in Hiroshima Synchrotron Radiation Center. Experimental energy resolution was set at 5 meV. The spectra were collected in vacuum better than 10^{-8} Pa and at a temperature of about 10 K, which is sufficiently below T_c.

The ARPES spectra were taken over a wavenumber region indicated by gray area in Fig. 1(b), where the solid curve denotes Fermi surface. Fermi angle, θ_{FS}, is defined around (π, π) point, so that θ_{FS} = 0° and 45° corresponds to nodal and antinodal directions, respectively. The symmetrized spectra at minimum-gap loci and energy-wavenumber plot of ARPES spectra were shown in Fig. 1(a) and Fig. 1(c) – (d), respectively. The data presented here were taken along four representative cuts as indicated by arrows in Fig. 1(b). Under the assumption of the particle-hole symmetry around Fermi energy E_F, symmetrizing a spectrum with respect to E_F is expected to cancel the Fermi cutoff. Figures 1(a), (c) and (d) show that the spectral peak remains below E_F except for the nodal cut, θ_{FS} = 0°, as evidence of the opening of *d*-wave-like superconducting gap. One can see from Fig. 1(a) that the gap disappears at θ_{FS} = 0°, and that the gap widens in going off the node toward the antinode. In order to quantitatively determine the magnitude of the gap, we fit the spectra for x = 0.01 and 0.04 with an empirical function given by Norman *et al*. [3]. The gap obtained at each direction was denoted by vertical bars in Fig. 1(a) and plotted against sin 2θ_{FS} in Fig. 2, where the present results for x = 0.01 (triangles) and 0.04 (circles) are compared with those of pristine sample (squares) from Ref. 4. Since sin 2θ_{FS} is adopted for the horizontal axis, the difference from the pure *d*-wave gap is easily seen from Fig. 2. We found that, in going toward the antinode, the gap of the Co-substituted samples starts to deviate from *d*-wave form around sin 2θ_{FS} ~ 0.3 and 0.4 for x = 0.01 and 0.04, respectively. This indicates that the antinodal gaps are larger than the linear extrapolation of the near-nodal gap. In addition, the near-nodal slope of the gap opening is almost unchanged with substitution of Co for Cu. However, the increase in the gap with Co substitution is found near the antinodal region. At the point of sin 2θ_{FS} = 0.5, the gaps of the Co-substituted sample are about 3 meV larger than that of the pristine sample. Even though T_c decreases from 91 K to 55 K with 4% substitution of Co for Cu, the decrease in near-nodal gap was insignificant. This indicates that the Co impurities does not affect the binding energy of Cooper pairs but reduce the density of Cooper pairs. The decrease in pair density is probably caused by the formation of pseudogap, which is consistent with our observation that the antinodal gap increases with Co substitution.

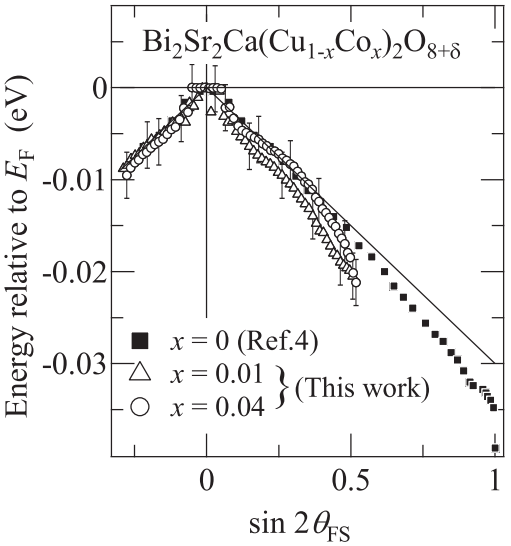

FIGURE 2. Directional dependence of the superconducting gap for $Bi_2Sr_2Ca(Cu_{1-x}Co_x)_2O_{8+\delta}$.

Taken together, we performed a laser-based high-resolution ARPES study on $Bi_2Sr_2Ca(Cu_{1-x}Co_x)_2O_{8+\delta}$. We observed that the gap widens in going off the node. Upon substitution of Co for Cu, the decrease in the near-nodal gap is insignificant, while the increase in antinodal gap is noticeable. These data suggest that the Co impurities do not affect the binding energy of the Cooper pairs but result in the reduction of the density of the Cooper pairs. The systematic gap study of the dependence on the amount of Co substitution would be helpful to reveal the relation between the superconductivity and the antiferromagnetic fluctuation in cuprates.

REFERENCE

1. J. Bardeen, L. N. Cooper, and J. R. Schrieffer, Phys. Rev. **108**, 1175 (1957).
2. A. Matsuda, T. Fujii, and T. Watanabe, Physica C **207**, 388–389 (2003).
3. M. R. Norman, M. Randeria, H. Ding, and J. C. Campuzano, Phys. Rev. B **57**, R11093–R11096 (1998).
4. H. Anzai, A. Ino, M. Arita, H. Namatame, M. Taniguchi, M. Ishikado, K. Fujita, S. Ishida, and S. Uchida, Nat. Commun. **4**, 1815 (2013).

One-Dimensional Surface Atomic Structure of Bi/InSb(001)

Y. Ohtsubo[a,b], J. Kishi[a], M. Nurmamat[c] and S. Kimura[a,b]

[a]*Graduate School of Frontier Biosciences, Osaka University, Suita 565-0871, Japan*
[b]*Department of Physics, Graduate School of Science, Osaka University, Toyonaka 560-0043, Japan*
[c]*Graduate School of Science, Hiroshima University, 1-3-1 Kagamiyama, Higashi-Hiroshima 739-8526, Japan*

Keywords: One-dimensional surface, atomic structure, Scanning Tunneling Microscopy

In recent days, low-dimensional electronic states derived from heavy elements with strong spin-orbit interaction are attracting attention in the field of solid-state physics because of its Dirac-cone-type dispersion with very steep dispersion and typical spin-orbital polarization without magnetic order [1]. Among them, the quasi-1D (Q1D) states in highly anisotropic materials are studied eagerly [2] because of high-efficient suppression of carrier backscattering (BS). Without BS, a new pathway to realize the dissipation-free high-speed conduction is expected.

Recently, we have found the InSb(001) surface covered with a few monolayers of Bi hosts the Q1D surface states with Dirac-like steep dispersion [3]. While such character is encouraging for the future applications mentioned above, the detailed information about the surface atomic structure had not been clear yet. In this project, we tried to reveal the surface atomic structure of the Q1D Bi/InSb(001) surface by using low-temperature scanning tunneling microscopy (LT-STM) equipment at HiSOR.

The Bi/InSb(001) surface was prepared *in-situ* in the preparation chamber attached to the LT-STM chamber. The InSb(001) substrates were cleaned by repeated cycles of Ar ion sputtering (ion energy around 1 keV) and annealing up to 680 K. Afterwards, 5-10 monolayers of Bi was evaporated at room temperature from a Knudsen cell. Surface atomic structures before and after the Bi evaporation were observed by low-energy electron diffraction (LEED) and the LT-STM at 77 K with constant-current mode.

Figure 1 shows the typical atomic-resolution STM image of the Bi/InSb(001) surface, showing 1D anisotropic surface structures. Needle-like 1D structures are made of two Bi atoms with the inter-atomic length (~4.5 □) close to those of the Bi single crystal. The 1D needles are aligned along the [110] direction of the InSb(001) substrate. The Dirac-like dispersion of the surface state was along the 1D needle-like structure shown here. Therefore, it is strongly suggested that the Q1D electronic state originates from these surface 1D structure.

Detailed theoretical calculations to reveal the origin of the Q1D Dirac-like states is in progress based on the surface atomic structure obtained in this project.

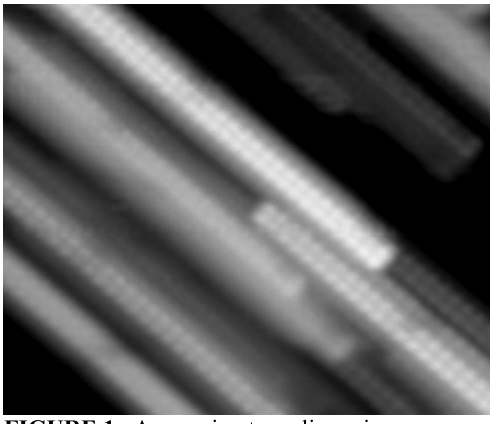

FIGURE 1. A scanning tunneling microscopy image of the Bi/InSb(001) surface (Bi coverage: 5 ML) taken at 77 K. Bias voltage and tunneling current were set at -0.10 V and 0.15 nA, respectively. The area of the image is 15×13 nm^2.

REFERENCES

1. M. Z. Hasan and C. L. Kane, *Rev. Mod. Phys.* **82**, 3045 (2010).
2. J. W. Wells *et al.*, *Phys. Rev. Lett.* **102**, 096802 (2009) and G. Autes *et al.*, *Nature Mat.* **15**, 154 (2016).
3. J. Kishi *et al.*, *submitted* (arXiv: 1704.05258 (2017)).

Electronic Structures of Hafnium Pentatelluride Studied by Micro-spot LaserARPES

M. Ye[a], H. Takita[b], E. F. Schwier[c], K. Shimada[c], W. Wang[d], L. He[d]

[a] *Shanghai Institute of Microsystem and Information Technology, Chinese Academy of Sciences*
[b] *Graduate School of Science, Hiroshima University*
[c] *Hiroshima Synchrotron Radiation Center, Hiroshima University*
[d] *School of Electronic Science and Engineering, Nanjing University*

yemao@mail.sim.ac.cn

Keywords: Topological semimetal; Topological insulator; ARPES;

Topological order in two-dimensional material has attracted intensive research interests as a potential platform for the quantum spin Hall effect (QSHE) [1, 2]. Very recently, the mono-layer of zirconium pentatelluride ($ZrTe_5$) and hafnium pentatelluride ($HfTe_5$) were predicted to host QSHE at high temperature, due to their relatively large band gap (~0.1 eV) [3]. And it was further predicted that the three dimensional bulk phase of $ZrTe_5$ and $HfTe_5$ may also show topological orders. However, the nature of the such topological orders are sensitively depending on the detailed calculation parameters, where the variation of lattice parameters leads to a transition between weak topological insulator and strong topological insulator for both $ZrTe_5$ and $HfTe_5$ [3]. On the experimental side, however, the transport measurement showed that $HfTe_5$ behaved as a Dirac semimetal with ultrahigh carrier mobility [4,5].

In order to clarify the topological natures of the bulk phase of $HfTe_5$, we perform angle-resolved photoemission spectroscopy measurement on $HfTe_5$ bulk crystals. By using brilliant UV laser light focused into micrometer-order spot, we are able to clearly probe the band structures of $HfTe_5$, and also the evolution of electronic states as a function of temperature.

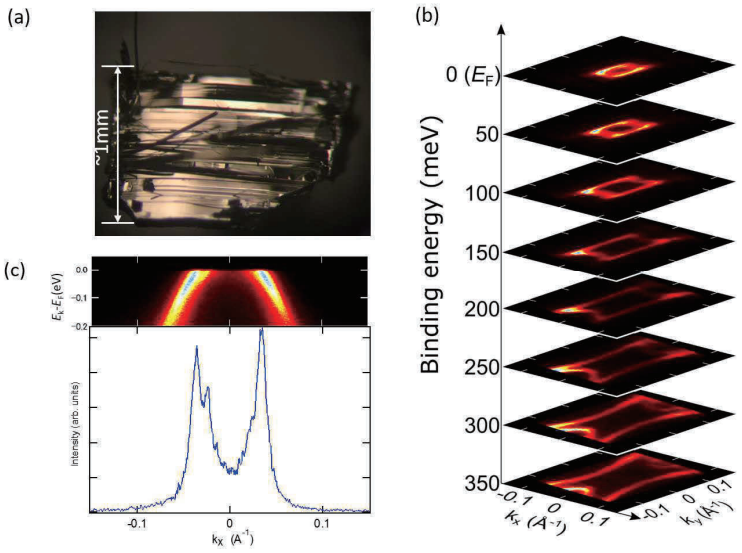

FIGURE 1. (a) Optical microscope photo of the cleaved surface of $HfTe_5$; (b) Constant energy contour of $HfTe_5$ around the Γ point; (c) Upper panel, energy band dispersion of $HfTe_5$ along Γ-X direction; lower panel, momentum distribution curve at the Fermi energy.

The photoemission measurement was performed at the laser ARPES station in Hiroshima Synchrotron Radiation Center, using the nonlinear second-harmonic generated ultraviolet as excitation photon source, which is focused down to micrometer-order size at sample position. The single crystalline $HfTe_5$ sample was cleave in ultrahigh vacuum by scotch tape, and quickly inserted into the liquid helium cryostats. Figure 1(a) shows the optical microscope photo of the $HfTe_5$ cleaved surface, which shows a large amount of narrow stripe domains with width less than 50 μm.

Figure 1(b) shows a series of constant energy contour of $HfTe_5$ around the Γ point acquired at 15 K, where a strongly anisotropic band structures was observed between Γ-X and Γ-Y directions, being in good consistence with theoretical calculations [3]. The detailed electronic states in the vicinity of Fermi energy is shown in Figure 1(c). One can clearly see that a pair of linear band structure approaching the Fermi energy, indicating that the measured samples held hole-type carriers. A close analysis of the electronic states reveals an addition states in the vicinity of Fermi energy, which can be further visualized in the momentum distribution curve as shown in the lower panel of Figure 1(c). These two sets of distinct states may be ascribed to the different origins from surface and bulk electronic states, indicating a strong topological order in bulk $HfTe_5$ phase [6].

REFERENCES

[1] M. Z. Hasan and C. L. Kane, Rev. Mod. Phys. **82**, 3045 (2010).
[2] X.-L. Qi and S.-C. Zhang, Rev. Mod. Phys. **83**, 1057 (2011).
[3] H. M. Weng, X. Dai, and Z. Fang, Phys. Rev. X **4**, 011002 (2014).
[4] H Wang, *et al.*, Phys. Rev. B **93**, 165127 (2016).
[5] L. X. Zhao, *et al*., arXiv:1512.07360 (2015).
[6] G. Manzoni, *et al*., Phys. Rev. Lett. **117**, 237601 (2016).

LASER ARPES of the Nematic Phase of FeSe

M. D. Watson,[a] A. A. Haghighirad,[b] H. Takita,[c] W. Mansuer,[c] H. Iwasawa,[a] E. F. Schwier,[d] A. Ino,[c,d] Y. Aiura,[e] and M. Hoesch [a]

[a]*Diamond Light Source, Harwell Campus, Didcot OX11 0DE, United Kingdom*
[b]*Clarendon Laboratory, Department of Physics, University of Oxford, Parks Road, Oxford OX1 3PU, United Kingdom*
[c]*Graduate School of Science, Hiroshima University, 1-3-1 Kagamiyama, Higashi-Hiroshima 739-8526, Japan*
[d]*Hiroshima Synchrotron Radiation Center, Hiroshima University, 2-313 Kagamiyama, Higashi-Hiroshima 739-0046, Japan*
[e]*National Institute of Advanced Industrial Science and Technology, Tsukuba 305-8568, Japan*

Keywords: laser-based ARPES, iron selenide

Since FeSe has a simplest crystal structure among iron-pnictides family, it provides a good opportunity to study the essential physics of its ordered phases. Specifically, FeSe exhibits tetragonal-orthorhombic "nematic" structural transition without any magnetic ordering, and thus it has been argued that orbital ordering may play a dominant role in the ordered phase. Experimentally, ARPES studies have been shown the splitting of d_{xz} and d_{yz} bands upon crossing nematic phase transition. However, the order parameter of the orbital ordering is yet to be determined because the interpretation of ARPES data has been still controversial with the size of splitting as well as the onset temperature of splitting.

Here we performed a laser-based ARPES to study the splitting of bands in the nematic phase of FeSe in detail. Experiments have been done in the laser-ARPES facility in HiSOR. Recently, optical lenses have been installed to the laser optics and μm-size laser spot are acquired. In addition to this, a half-wave plate is installed so that polarization can be changed from *s*- to *p*-polarization continuously.

Figure 1 show representive ARPES spectra at T = 15 K taken along high symmetry cut, showing that all the bands are nicely observed with mixed polarization while d_{xz} bands are mainly observed with *p*-polarization. As shown in the EDC around the Γ point, the energy of the d_{xy} and d_{yz} bands can be extracted from data taken with mixed polarization. With in-depth analysis using spectrum divided by the Fermi-Dirac function, energy of the d_{xz} band can also be extracted. We have performed a temperature dependence study with mixed polarization and observed a splitting of the d_{xz} and d_{yz} bands by magnitudes of 13 meV and a downward shift of d_{xy} band with the onset of T = 90 K. These results are associated with a symmetry-breaking orbital ordering.

In summary, we performed a laser-based ARPES study of FeSe in detail and observed that shift of hole-like bands around the Γ point, revealing the onset of splitting of d_{xZ} and d_{yz} bands below 90 K. In addition the d_{xy} band also shift to higher binding energy at 90 K. These results help the theoretical study of the nematic order in FeSe.

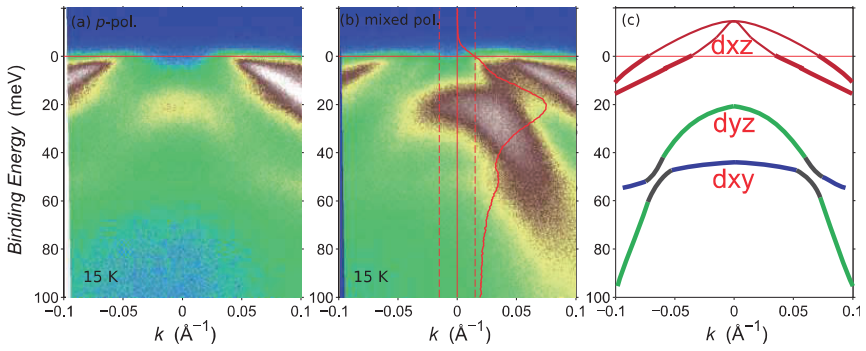

FIGURE 1. (a)(b) ARPES spectra along the high symmetry line at T = 15 K taken with *p*- and mixed polarization, respectively. The EDC in mixed polarization data is extracted along k = 0 with an integration window of 0.015 Å^{-1} shown by dotted red lines. (c) schematic band structure of FeSe.

Resolving the complex low-energy electronic structure of the quasi-one-dimensional material $NbSe_3$

Claude Monney[a], Eike F. Schwier[b], C.W. Nicholson[c] and M. Hoesch[d]

[a]*Physics Department, University of Zurich, Winterthurerstrasse 190, Zurich 8057, Switzerland*
[b]*Hiroshima Synchrotron Radiation Center (HSRC), Hiroshima University, Higashi-Hiroshima 739-0046, Japan*
[c]*Department of Physical Chemistry, Fritz-Haber-Institut, Faradayweg 4-6, Berlin 14915, Germany*
[d]*Diamond Light Source, Harwell Campus, Didcot OX11 0DE, Oxfordshire, United Kingdom*

Keywords: Tomonaga-Luttinger liquid, charge density wave phase, angle-resolved photoemission spectroscopy.

Quasi-one-dimensional (1D) materials have received much attention in recent years due to both their potential technological uses and as systems, which may display exotic low-dimensional physics such as the Tomonaga-Luttinger liquid (TLL) phase [1,2]. A case in point is the quasi-1D material $NbSe_3$. It is one of the few materials that exhibits all the ingredients of a charge density wave (CDW) i.e. resistivity anomalies; a periodic lattice distortion and sliding density waves, which carry an electric current. $NbSe_3$ exhibits two CDW transitions at 145 K and 59 K [3]. While $NbSe_3$ has been intensively investigated from a transport and lattice point-of-view, the electronic structure, by comparison, has been hardly studied so far [4,5].

We have recently performed a high-energy-resolution angle-resolved photoemission spectroscopy (ARPES) experiment at Diamond Light Source and measured the full Fermi surface of NbSe3 [6]. According to density functional theory (DFT), its low energy electronic structure consists of 5 bands, which we could hardly resolve. We have also observed an anomalous depletion of spectral weight close to the Fermi level, which resembled that expected for a TLL phase. However in order to study the possibility of the occurrence of a TLL, we had to integrate all 5 bands over momentum to look for a power-law depletion of the total density of states (DOS) near the Fermi level.

In the current experiment, we have taken advantage of both the very small spot of the laser beam and the very high momentum- and energy-resolution of the laser ARPES setup at HiSOR to achieve measurements of unprecedented quality. This allows us to resolve all 5 bands of $NbSe_3$ and to compare their specific contribution to the DOS in order to understand whether they are affected differently by the TLL physics at play in $NbSe_3$. Furthermore, we are able to observe for the first time the CDW gap taking place at E_F in the inner bands of $NbSe_3$.

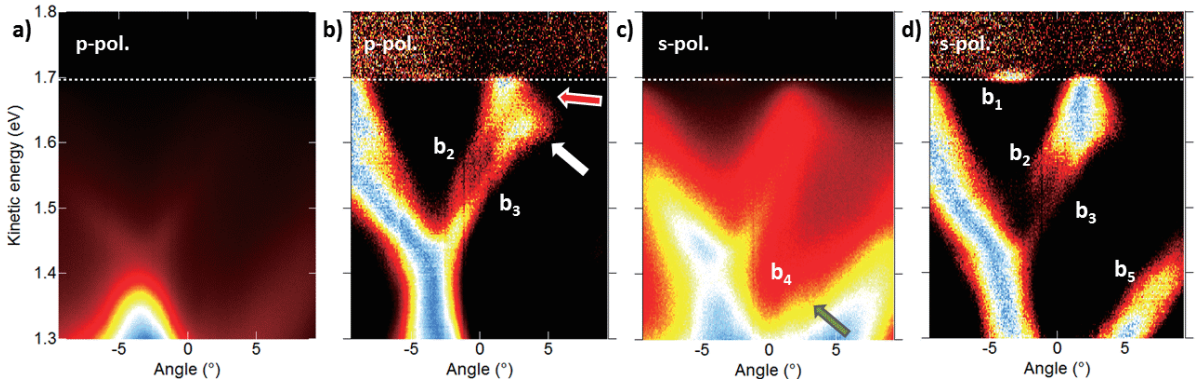

FIGURE 1. ARPES data of $NbSe_3$ measured at 24 K near the Γ point with different linear light polarization. (a) Raw data and (b) processed data (each MDC height-normalized after a constant background subtraction) with *p*-polarized light. (c) Raw data and (d) processed data with *s*-polarized light. The position of the Fermi edge is indicated with the horizontal white dashed line.

Figure 1 shows typical high-resolution ARPES data taken with the laser ARPES setup. During this beamtime, the laser photon energy was set to 197 nm, meaning 6.29 eV. At first look, the effect of light polarization is very strong, such that it is difficult to see the low-energy dispersions with *p*-polarized light (graph (a)). Therefore, we process the raw data by subtracting a constant intensity background along each momentum distribution curves (MDC), which are then normalized to their maximum height. This highlights the relevant dispersions, as shown in graph (b). The same procedure is applied to the raw data obtained with *s*-polarized light (see graphs (c) and (d), respectively). Looking at the processed data, graphs (b) and (d), one distinguishes the 5 bands predicted by DFT and labelled b_1 to b_5. Interestingly, band b_3 is not reaching the Fermi level and bends downwards, as indicated by the white arrow in graph (b). This is the indication of a CDW gap opening at the Fermi level (red arrow), which is clearly observed for the first time here for $NbSe_3$. It explains how the CDW phase is stabilized in this material, by lowering the energy of the corresponding states. Similar data have been taken at different emission angles at low temperature to map the evolution of the bands in the vicinity of the Γ point. This reveals more clearly band b_4, hardly visible in Figure 1(c) (green arrow), likely due to emission angle dependence of the matrix elements.

Finally, we have also measured data near Γ for different temperatures up to 170 K. These data are currently under analysis. This will lead to two important results. First, the CDW gap will be followed as a function of temperature. Second, we will perform a temperature dependent analysis of the spectral weight depletion in bands b_2 and b_3. This will be related to the physics of the dimensional crossover occurring in $NbSe_3$ [6]. We will clarify whether the CDW vs TLL physics is taking place in specific bands in this material.

The $NbSe_3$ samples have been grown by H. Berger (Institut de la Matière Complexe, Ecole Polytechnique Fédérale de Lausanne, Lausanne 1015, Switzerland).

REFERENCES

1. S. Tomonaga, Prog. Theor. Phys. 5, 544 (1950).
2. J. M. Luttinger, J. Math. Phys. 4, 1154 (1963).
3. P. Monceau, Adv. Phys. 61, 325 (2012).
4. J. Schaefer, E. Rotenberg, S. D. Kevan, P. Blaha, R. Claessen, and R. E. Thorne, Phys. Rev. Lett. 87, 196403 (2001).
5. J. Schaefer, M. Sing, R. Claessen, E. Rotenberg, X. Zhou, R. Thorne, and S. Kevan, Phys. Rev. Lett. 91, 066401 (2003).
6. C. W. Nicholson, C. Berthod, M. Puppin, H. Berger, M. Wolf, M. Hoesch and C. Monney, accepted for publication in Phys. Rev. Lett., arXiv: 1610.05024.